Metrical oxidation states of 1,4-diazadiene (DAD) derived ligands

*Felix J. de Zwart, Bente Reus, Annechien A.H. Laporte, Vivek Sinha and Bas de Bruin**

Van 't Hoff Institute for Molecular Sciences, University of Amsterdam, 1098 XH Amsterdam,
The Netherlands

1,4-diazadiene, redox-active ligands, (electronic) structure, (transition) metals, oxidation states

ABSTRACT: The conventional method of assigning formal oxidation states (FOS) to metals and ligands is an important tool for understanding and predicting chemical reactivity, in particular in catalysis research. For complexes containing redox-noninnocent ligands, the oxidation state of the ligand can be ambiguous (i.e. their spectroscopic oxidation state can differ from the formal oxidation state), and thus frustrates the assignment of the oxidation state of the metal. A quantitative correlation between empirical metric data of redox active ligands and their oxidation states using a metrical oxidation state (MOS) model has been developed for catecholate and aminophenolate derived ligands by Brown. In the present work, we present a MOS model for 1,4-diazabutadiene (DAD^n) ligands. The model is based on a similar approach as reported by Brown, correlating the intra-ligand bond lengths of the DAD^n moiety in a quantitative manner to the MOS using geometrical information from X-ray structures in the Cambridge Crystallographic Data Center (CCDC) database. However, accurate determination of the MOS of these ligands turnedout to be dependent the coordination mode of the DAD^{2-} moiety, which can adopt both a planar κ^{2}-N_{2}-geometry and a η^{4}-$N_{2}C_{2}$ π-coordination mode in (transition) metal complexes in its doubly reduced, dianionic enediamide oxidation state. A reliable MOS model was developed taking the intrinsic differences in intra-ligand bond distances between these coordination modes of the DAD^{2-} ligand into account. Three different models were defined and tested using different geometric parameters (C=C→M distance, M–N–C angle, M–N–C–C torsion angle) to describe the C=C backbone coordination to the metal in the η^{4}-N_{2}-C_{2} π-coordination mode of the DAD^{2-} ligand. Statistical analysis revealed that the C=C→M distance best describes the η^{4}-N_{2}-C_{2} coordination mode, using a cut-off value of 2.46 Å for π-coordination. The developed MOS model was used to validate the oxidation state assignment of elements not contained within the training set (Sr, Yb and Ho), thus demonstrating the applicability of the MOS model to a wide range of complexes. Chromium complexes with complex electronic structures were also shown to be accurately described by MOS analysis. Furthermore, it is shown that a combination of MOS analysis and FOD calculations provide an inexpensive method to gain insight into the electronic structure of singlet spin state ($S = 0$) [M(trop$_{2}$dad)] transition metal complexes showing multireference character.

1. Introduction

Assigning oxidation states to metals and ligands is an important tool in the field of inorganic chemistry to understand and predict chemical reactivity. In particular understanding the concepts of homogeneous catalysis strongly relies on electron counting and oxidation state assignments. The conventional method for assigning oxidation states concerns the use of *formal oxidation states* (FOS), in which the ionic character of all bonds is exaggerated. This is a particularly useful tool for bookkeeping of electrons in redox reactions. However, the formal oxidation state is not a measurable quantity but an axiomatic formalism and in complexes that have electronic structures not properly described by an ionic approximation the FOS does not reflect the real (spectroscopic) electronic density distribution of the complex. Limitations to the formal oxidation state concept have long been described in literature, stemming from inconsistencies in FOS rules and problematic organometallic cases.[1,2,3] In particular, redox active ligands and complexes thereof have time and again proven to have electronic structures not accurately described by formal oxidation states. The *physical oxidation state* of a metal can be thought of as a continuous electronic-structure descriptor that reflects the electron density distribution around the metal center in a transition metal complex.[4] The physical (or spectroscopic) oxidation state of the metal center in a complex can be inferred through several spectroscopic methods and only a multi-technique approach allows comprehensive understanding of the electronic structure. For the oxidation state of redox-active ligands in particular, the geometric information obtained from crystal structures has been used to deduce the ligand oxidation state and by proxy the metal oxidation state. In practice this is generally done by qualitatively comparing a newly acquired crystal structure to structures in literature with known electronic structures.[5] Statistical analysis of crystal structures is a growing field within chemistry, and has particular strengths in highlighting trends that might not be visible by looking at a single crystal structure.[6,7] More specifically, statistical research using the Cambridge Structural Database (CSD) has been used to enhance chemical understanding of bond conformations,[8,9] discover new bonding interactions,[10] improve computational methods,[11] and to better understand metal-ligand interactions.[12,13] In the case of redox-active ligands (or redox-noninnocent ligands), large literature surveys in combination with computational methods have been used to gain insight into continuous bond deformations as a function of oxidation state.[14] In 2012, a seminal article by Brown made important steps to quantifying the relationship between the geometric information of catecholate and amidophenoxide ligands through defining a *metrical oxidation state (MOS)*, which is a continuous (integer or non-integer) variable describing the oxidation state of the ligand.[15] By using least-squares fitting of ligand bond lengths, the oxidation state of a newly acquired crystal structure can be determined without having to resort to literature comparison to selected structures. Following this approach, Brown quantified the well-known intra-ligand metrical changes of catecholate and aminophenoxide ligands within a single parameter, and the thus obtained MOS provides a convenient handle to assign ligand oxidation states in a quantitative manner. Metrical oxidation state calculations were subsequently used to confirm various oxidation state assignments of newly synthesized complexes.[16]

Herein, we present the development of a related model for redox-active 1,4-diazabutadiene-type ligands (Figure 1a).

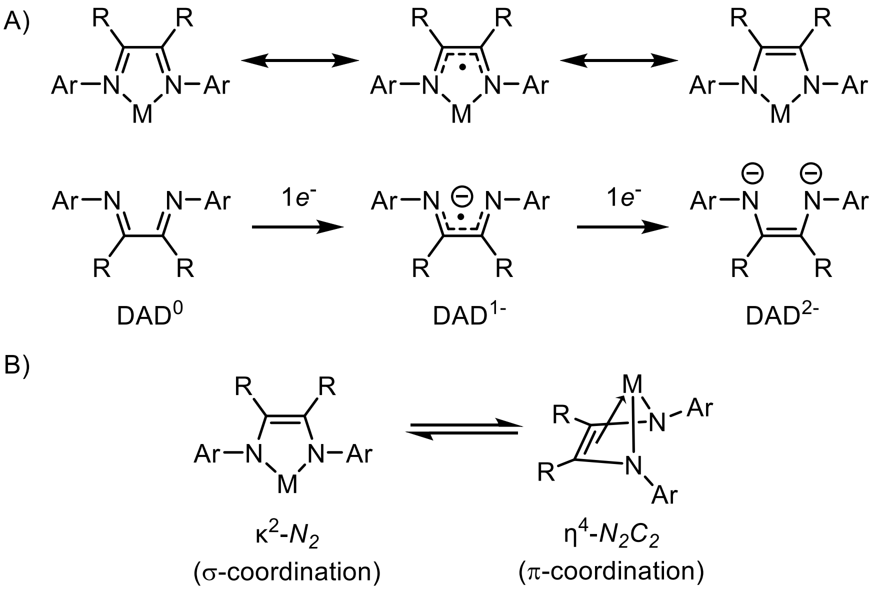

Figure 1. (a) Accessible oxidation states of the diazabutadiene ligand framework. Neutral diimine (left), one-electron reduced semi-iminato (middle) and fully reduced enediamide (right) forms. (b) κ^2-N_2 (left) and η^4-N_2C_2 (right) binding modes of the fully reduced enediamide form. R= H, CH_3.

The treatment of the fully reduced enediamide form is of particular interest as it is known to bind in both κ^2-N_2 and η^4-N_2C_2 manners (Figure 1b). Rearrangement from σ- to π-coordination has been shown to facilitate elementary steps in catalytic cycles of DAD^{2-} complexes.[17,18] These geometrical differences also give rise to differences in the intra-ligand bond lengths, which is of prime importance for the MOS model developed in this paper. As such, we evaluated various geometric descriptors for the treatment of both binding modes in a single model. The flexible π-coordination of the enediamide C=C backbone leads to a distortion in the planarity of the ligand, and subsequently we hypothesized that the C=C→M distance, M−N−C bond angle and M−N−C−C torsion angles could be valid descriptors of the η^4-N_2C_2 binding mode.

2. Methods

In order to establish a metrical oxidation state model for the DAD ligand framework, an initial dataset was created using complexes reported in the Cambridge Structural Database (CSD) for which the physical oxidation state is unambiguously characterized in the available literature. Particular care was taken in selecting a wide variety of complexes to reduce any bias in the dataset. Figure 2 contains a list of all metal centers with at least one entry in the final dataset. A consistent set of criteria was set up in order to ensure the integrity of the dataset, excluding complexes in which the ligand framework coordinates to multiple metal centers, metal cluster compounds and complexes in which the DAD moiety is part of a higher denticity ligand. X-ray structures with unusually large ellipsoids, metal centers on symmetry axes or other crystallographic issues such as checkCIF alerts were manually excluded. The geometric parameters of these complexes were collected from the Cambridge Structural Database (CSD) version 5.41 (November 2019) using the ConQuest tool version 2.0.4 (build 270009).[19,20] This provided 147 crystallographic distinct entries for neutral diimine ligands (DAD^0), 43 entries for one-electron reduced semi-iminato ligands (DAD^{1-}), and 64 entries for fully reduced enediamide ligands (DAD^{2-}).

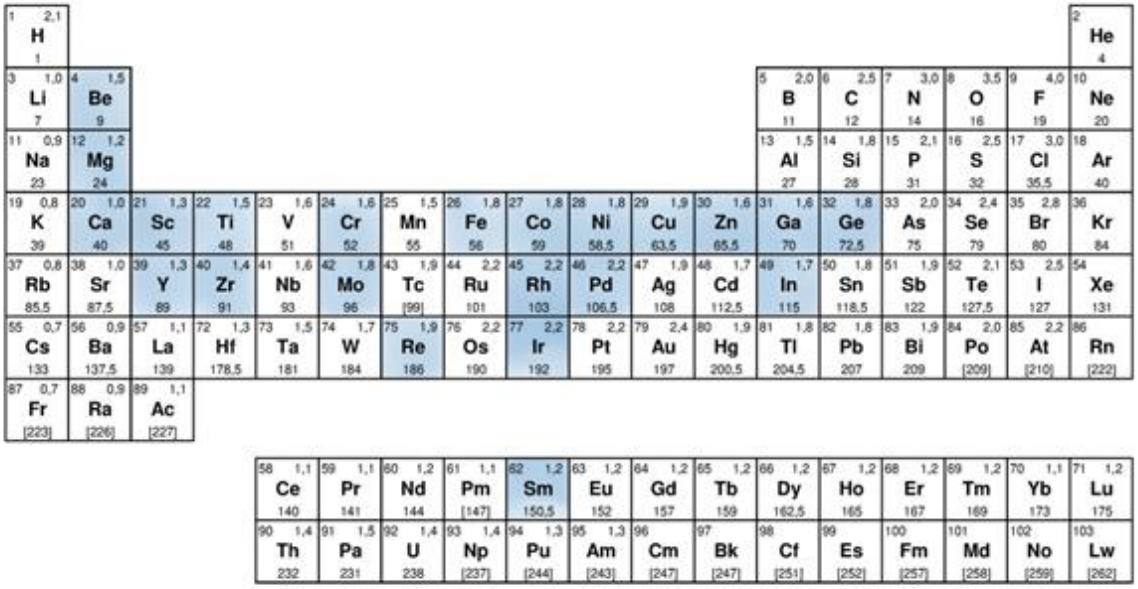

Figure 2. Metal complexes included in the dataset containing 1,4-diazabutadiene ligands, with final selected elements highlighted in blue.

The average C−N and C−C bond lengths of the DAD ligands in the selected complexes were plotted as a function of the reported DAD^{n-} ligand oxidation states, and subsequently fitted to a linear relationship for the C−N bond length and a quadratic relationship for the C−C bond length (Figure 3). The metrical oxidation state of each ligand was calculated by unweighted least-squares fitting (for details see supporting information), minimizing the sum of squares of the difference between the observed bond lengths and the calculated bond lengths from the functions derived from the training set. The minimization of the least-squares fitting was applied with the Levenberg−Marquardt algorithm as presented in Microsoft Excel. To determine the error of the calculated MOS values, an estimated standard deviation (esd) was computed for each structure. The esd values were calculated using the typical formula for the estimated standard deviation with an additional factor for the propagation of error, which was based upon the standard error of the observed bond lengths. The calculated MOS values were tested on normality by Shapiro-Wilk Extended (SWE) tests.

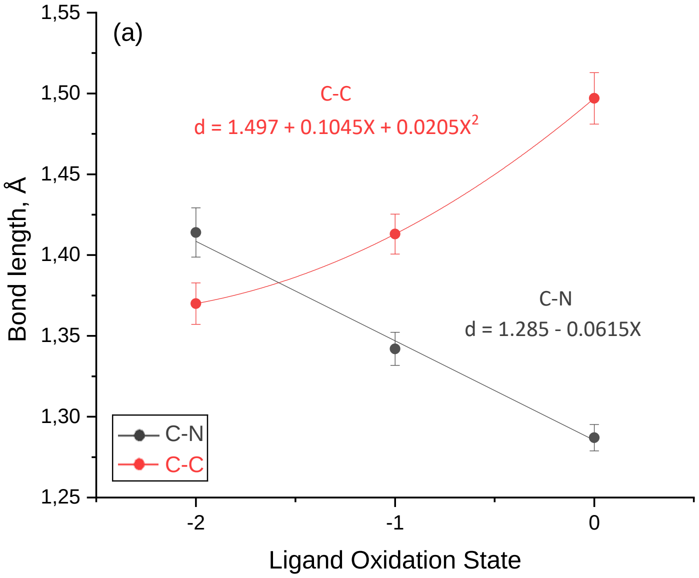

Figure 3. DAD bond distances as a function of the reported DAD ligand oxidation states. For exact values of the C–C and C–N bond lengths as a function of literature reported ligand oxidation state see Table 3.

The calculated MOS values were evaluated on the basis of their distribution around and deviation from the literature assigned oxidation states. All calculated MOS values can be found in Supporting Information spreadsheet “MOSCalculator.xlsx”, and all MOS distribution histograms and boxplots can be found in the ESI. For none of the models any overlap between the calculated MOS values of the DAD^n ligands ($n = 0, 1-, 2-$) is visible in the box plots, which was confirmed ($p < 0.05$) by Grubbs tests. The spread of the neutral diimine (DAD^0) and one-electron reduced semi-iminato (DAD^{1-}) ligand is small, and the datasets do not overlap at all (Figure 4). The MOS calculated for the DAD^0 complexes in the data set are found in a range between +0.3 and –0.4, with a clear peak at 0 and most complexes having a MOS between +0.1 and –0.1. The MOS calculated for the DAD^{1-} complexes in the data set are found in a range between –0.6 and –1.3, with a clear peak at –1 and most complexes having a MOS between –1.1 and –0.9. These data suggest that most DAD^0 and DAD^{1-} ligands have integer oxidation states (n= 0 or n= −1), with only a few exceptions pointing to possible non-integer ligand oxidation states. While the dataset of the fully reduced DAD^{2-} ligand doesn't overlap with the DAD^{1-} dataset (Figure 4), it is clear that the spread is broader and differs for each geometry descriptor. The MOS calculated for the DAD^{2-} complexes in the data set are found in a range between –1.5 and –2.6, in two sections: A data section between –1.5 and –2.0 (most data between –1.6 and –1.8) and a data section between –2.0 and –2.6 (most data between –2.1 and –2.3). The broader spread of calculated (uncorrected) MOS observed for the fully reduced DAD^{2-} ligand is not (primarily) caused by a larger number of complexes with non-integer ligand oxidation states (i.e. deviations from n = –2), but rather to a distribution of DAD^{2-} complexes different binding modes. A majority of complexes with a κ^2-N_2-DAD^{2-} binding mode, a smaller number of complexes with a η^4-N_2C_2-DAD^{2-} binding mode and some in between, each giving rise to MOS values deviating somewhat from –2. This leads to deviations in the calculated MOSs if left untreated, as the intra-ligand bond distances of the η^4-N_2C_2-DAD^{2-} ligands are quite different from those in the κ^2-N_2-DAD^{2-} ligands (especially the C–N distances, see Table 1). This would lead to overestimation of the metrical oxidation state of the κ^2-N_2-DAD^{2-} ligands and underestimation of the metrical oxidation states of the η^4-N_2C_2-DAD^{2-} ligands. Hence, we decided to modify the MOS model to correct for this fact, in which the MOS of the DAD^{2-} ligand is calculated based on a weighted contribution of κ^2-N_2- and η^4-N_2C_2 binding modes (see below). Understanding the flexible backbone of the DAD^{2-} ligand is of particular interest, as π-coordination of the C=C backbone has been shown to play a critical role in lowering activation barriers in catalysis.[17,18]

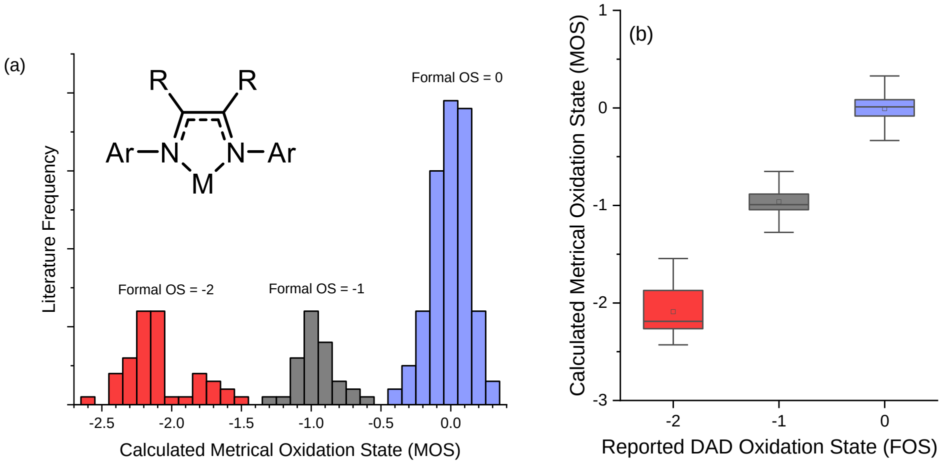

Figure 4. Distribution of calculated metrical oxidation states for the initial dataset without separate treatment of the enamide κ^2-N_2-DAD^{2-} and η^4-N_2C_2-DAD^{2-} binding modes as (a) histogram and (b) boxplot. (MOS= 0: Range between +0.3 and –0.4; MOS= –1: Range between –0.6 and –1.3; MOS= –2: Broad range between –1.5 and –2.6, split into two smaller distributions; one distribution between –1.5 and –2.0 and another one between –2.0 and –2.6).

For the neutral diimine (DAD^0) and mono-anionic semi-iminato (DAD^{1-}) oxidation states of the ligand no special data treatment was required, as for those only the κ^2-N_2 binding mode is observed.[21] The geometrical parameters that were considered relevant to capture the η^4-N_2C_2-DAD^{2-} geometries are the C=C centroid-to-metal distance (C=C→M), the M–N–C bond angle and the M–N–C–C torsion angle. The M–C–C–N torsion angle provided results nearly identical to the M–N–C–C torsion angle. These parameters were collected for all structures and their distributions were fitted to two gaussian curves, from which a π-coordination cut-off value d_{avg} was determined (Fitted curves in Supporting Information S1, cutoff values in Table 1) with an accompanying estimated standard deviation based on the pooled variance. Based on the cut-off value, the DAD^{2-} dataset was split based on the binding modes leading to two different average C–N and C=C bond lengths. Each cut-off value led to significantly different averaged C–C and C–N bond length datasets ($p < 0.05$) for the two different DAD^{2-} binding modes.

Table 1. Cut-off values and resulting average bond lengths of the DAD^{2-} ligand in η^4- and κ^2-binding modes found in the data set.

Descriptor	C=C→M distance (Å)	M–N–C angle (°)	M–N–C–C torsion angle (°)
Cut-off value (d_{avg}) ± esd_d	$< 2.46 \pm 0.09$: η^4-N_2C_2 $> 2.46 \pm 0.09$: κ^2-N_2	$< 98.96 \pm 2.95$: η^4-N_2C_2 $> 98.96 \pm 2.95$: κ^2-N_2	$< 19.91 \pm 3.71$: κ^2-N_2 $> 19.91 \pm 3.71$: η^4-N_2C_2
Resulting average bond distances using the above different cutoff parameters:			
η^4 C–N average (Å) $^{(a)}$	1.3958	1.4051	1.4070
κ^2 C–N average (Å) $^{(a)}$	1.4173	1.4180	1.4165
η^4 C=C average (Å) $^{(a)}$	1.3743	1.3712	1.3701
κ^2 C=C average (Å) $^{(a)}$	1.3618	1.3560	1.3530

$^{(a)}$ Averaged intra-ligand bond distances of the DAD^{2-} ligand in the assigned η^4 and κ^2 binding modes, depending on the selections determined by the three indicated descriptors and cutoff values as listed at the top of each column.

Correlations between the DAD intra-ligand bond length and the reported DAD^{n-} oxidation states were again made using a linear relationship for the C=C bond lengths and a quadratic relationship for the C–N bond lengths. This led to two separate fits for the κ^2- and η^4 binding modes for each geometric descriptor (see Supporting Information S2), which were incorporated into a single metrical oxidation state calculation using the cumulative distribution function of the geometric descriptors (bond length, bond angle, torsion angle) as a weight factor WF according to equation 1. This weight factor determines what percentage of the κ^2 and η^4 fit is incorporated into the MOS calculation. Other ways of weighing the κ^2 and η^4 models were evaluated as well, such as taking the weighted descriptor average and using a discrete cutoff value, but the sigmoidal function best describes the continuous physical picture of π-coordination.

$$(1)\ WF = \frac{1}{esd_d\sqrt{2\pi}} e^{-\frac{1}{2}(\frac{d_{obs}-d_{avg}}{esd_d})^2}$$

WF = weighting factor; esd_d = estimated standard deviation of geometric descriptor; d_{obs} = observed descriptor value; d_{avg} = descriptor cutoff value.

In order to evaluate the performance of the geometry descriptors to describe the η^4-N_2C_2-DAD^{2-} coordination mode with C=C→M backbone coordination, two MOS performance criteria were evaluated (Table 2): (1) The average MOS value, which describes the accuracy of the model and should be as close to −2.000 as possible, and (2) the standard deviation describing the precision. While all descriptors provide a comparable accuracy, the precision of C=C→M distance as a descriptor outperforms the M–N–C angle and the M–N–C–C torsion angle, which is also visible in the histograms (Supporting Information S3).

Table 2. Performance criteria of selected geometric descriptors.

Descriptor	Average MOS in the DAD^{2-} dataset	Estimated standard deviation of the MOS
C=C→M distance	−2.020	0.16
M−N−C angle	−2.025	0.23
M−N−C−C torsion angle	−2.026	0.24

Prior to this investigation we expected all complexes containing a bent DAD ligand to contain a metal-backbone interaction. The difference in precision of the models prompted us to investigate which complexes were selected as η^4 by their deviation from planarity, but still had a large C=C to metal distance. The discrepancy in the descriptor performance seemed to stem from a set of samarium and yttrium complexes which contain a large C=C→M distance (2.63 ± 0.08 Å), but also a bent ligand (ω = 33.8 ± 3.6 °). Put into chemical terms, this means that judging from the bond distance, the DAD^{2-} ligand in these complexes is ligated in the κ^2 binding mode but judging from the ligand planarity the enediamide ligand is coordinated in η^4 fashion. Looking at the average C−N (1.420 Å) and C=C (1.366 Å) bond lengths, these complexes contain ligands that are described as predominantly κ^2. We propose that either a weak C=C→M interaction causes a large deviation of ligand planarity (e.g. due to the large ionic radii of these metals) or other effects such as crystal packing can cause bending of the DAD^{2-} ligand. The former hypothesis is supported by the larger distribution of interference of the C=C→M distances, (27% vs 5%), making it a more continuous descriptor compared to the M−N−C−C torsion angle, which is either flat (6 °) or bent (34 °). However, solid state crystal packing effects cannot be ruled out as the cause of a large torsion angle. Based on the performance metrics and the MOS normality the distance between the C=C bond and the metal center best describes the metal-backbone interaction. Satisfyingly, this is in agreeance with chemical intuition. The average C=C→M distance for η^4-N_2C_2-DAD^{2-}coordinated structures is 2.33 ± 0.07 Å. As such, this statistical analysis allows us to put a number on C=C→M π-coordination of the DAD^{2-} ligands, which could be of broader interest.

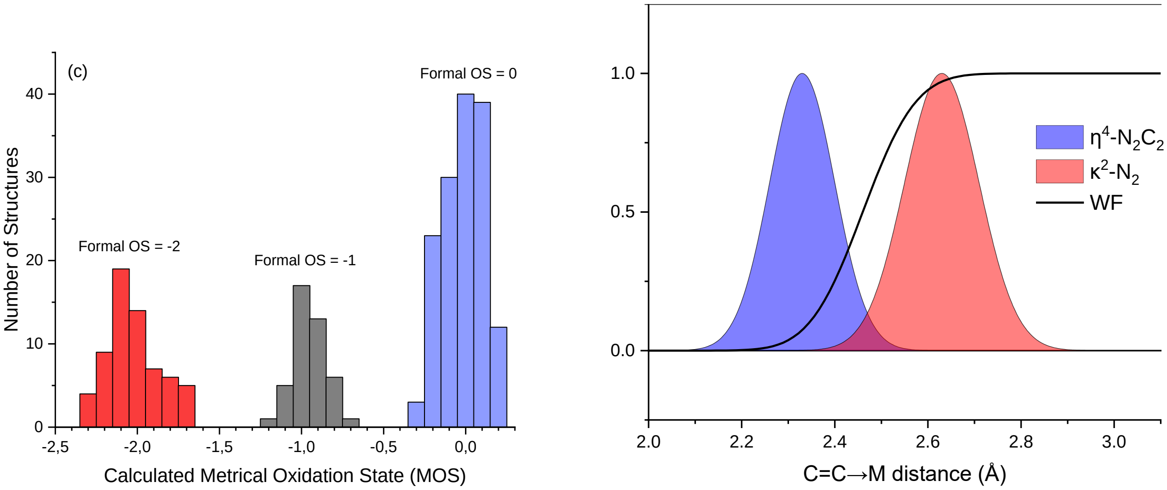

Figure 5. (a) Distribution of calculated metrical oxidation states using the C=C→M distance as a weight factor to describe enamide κ^2-N_2-DAD^{2-} and η^4-N_2C_2-DAD^{2-} binding modes. (b) Fitted distributions of the C=C→M distance in η^4-N_2C_2-coordinated and κ^2-N_2-coordinated structures.

Deviations of the metrical from the literature assigned oxidation state greater than 0.25 units are rare (4.2%), and the average residual sum of squares for each model was in the order of 10^{-3} confirming the efficacy of describing the ligand oxidation state through the bond lengths. This survey also provided the average C–C and C–N bond lengths for the ligand framework depending on the ligand oxidation state and binding mode, which seems largely independent of the metal oxidation state and is tabulated in Table 3.

.

Table 3. Average bond lengths for C−C/C=C and C−N bonds in metal DAD^n complexes as a function of literature assigned ligand oxidation states.

Ligand oxidation state n (number of entries in the CSD)	C−N average ± stdev	C−C / C=C ± stdev
0 (147)	1.2853 ± 0.0075	1.4932 ± 0.017
−1 (43)	1.3420 ± 0.0088	1.4060 ± 0.012
−2 η^4 (25)	1.3958 ± 0.010	1.3743 ± 0.009
−2 κ^2 (39)	1.4173 ± 0.011	1.3618 ± 0.013

3. Results and Discussion

With the MOS model in hand, which accurately describes both η^4 and κ^2 binding modes of DAD^{2-} and the three oxidation states of the DAD ligand, the next step was to validate the model with various compounds outside of the training set. When developing the training set, care was taken to incorporate a wide range of elements as to create a model applicable to all DAD complexes regardless of the metal center. In order to validate whether the developed model provides satisfactory results for any metal, the metrical oxidation states for six DAD complexes of elements not contained within the training set (Sr^{II}, Ho^{III}, Yb^{III}) were calculated (Figure 6). The computed MOS values all provide results well within the ± 0.3 range of the literature assigned oxidation states. The two ytterbium complexes containing a DAD^{2-} ligand are described in literature as having a weak interaction with the C=C backbone.[23] From the C=C→M distance (2.530 Å and 2.536 Å respectively) it is expected that there is a slight interaction that influences the C=C and C–N bond lengths. Indeed, the weight factor (0.78 and 0.80) indicates that these complexes are predominantly κ^2-N_2-DAD^{2-}. For comparison, we calculated the MOS value with WF = 1, to validate the approach of using the C=C→M distance to incorporate weak backbone interactions into the MOS model. This indeed provided MOS values further away from the literature assigned oxidation state which shows that even when the backbone-metal interaction is weak, the sigmoidal weight function improves the accuracy of the metrical oxidation state calculation.

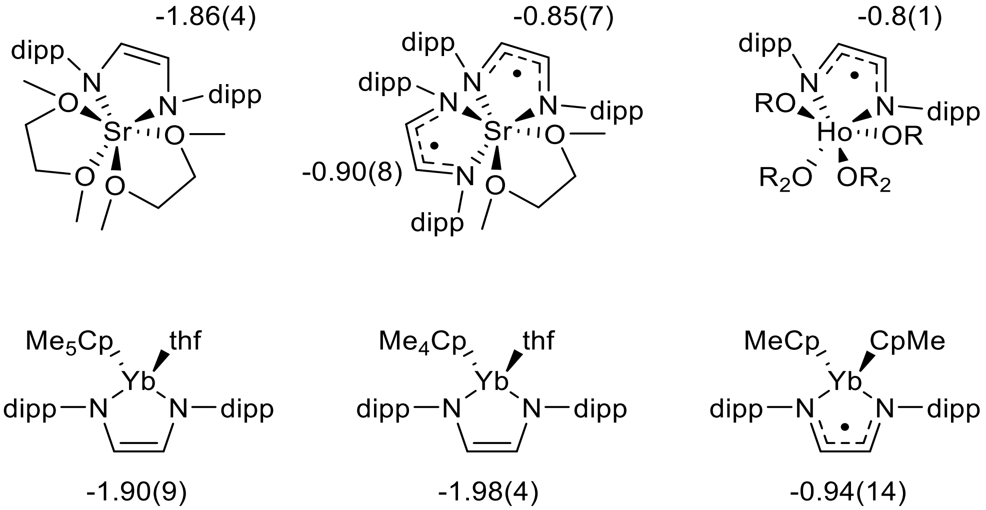

Figure 6. Sr, Ho and Yb complexes containing the DAD^{n} moiety.[22,23] For the holmium complex the siloxane cluster is not shown (dipp = 2,6-diisopropylphenyl, thf = tetrahydrofuran). Calculated metrical oxidation states are listed next to the ligand, with the model error in brackets. Crystallographic inequivalent entries were calculated separately and their MOS values were averaged and the error in the model was pooled.

In the amidophenoxide training set of Brown, three complexes with ligand formal oxidation state −1.5 were included, which can be interpreted as two ligands with overall charge −3 containing a radical delocalized over both ligands. In our studies we only came across a single complex which can be described as a complex with mixed oxidation state DAD^{n-} ligands. The anionic chromium(II) complex shown in Figure 7 was published in 2008 by Theopold *et al.*, who characterized the electronic structures of several chromium complexes in detail.[24] For

$[Cr(^{dipp}DAD)_2][Li(thf)_4]$, a quartet spin ground state was found by magnetic measurements, and for which DFT analysis revealed a Cr(II) center with one ligand-centered radical anion. This leads to an overall description of the complex as containing two DAD ligands with overall cumulative oxidation state −3, and thus individually −1.5, as the orbitals are not localized on either ligand. The mean MOS value of this complex calculated with our model (−1.65 ± 0.11) is in excellent agreement with this description. While not enough complexes were available to reliably include fractional oxidation states in the training set, we postulate that the model is robust enough to describe such cases.

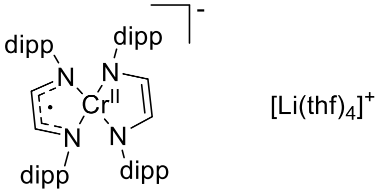

Figure 7. Homoleptic chromium(II) DAD complex $[Cr(^{dipp}DAD)_2][Li(thf)_4]$ best described as ligand oxidation state $DAD^{1.5-}$.

When developing the training set, we opted to leave out a set of five semi-iminato chromium(II) complexes due to the potential semi-iminato/enediamide $Cr^{II/III}$ ambiguity, and only include chromium(III) complexes. However, the electronic state of these five structures is strongly supported by spectroscopic and computational techniques as a Cr^{II}/DAD^{1-} oxidation state assignment.[25] The mean MOS values calculated for the 9 crystallographically inequivalent DAD ligands (−1.15 ± 0.21) is in satisfactory agreement with the assignment of these complexes as Cr^{II}/DAD^{1-}.

Electronic structure of [M(trop$_2$dad)] complexes.

Due to the exclusion of DAD ligands with a higher denticity from the MOS training set, the trop$_2$dad ligands were excluded from the training set. However, this ligand has seen widespread adoption in iron and ruthenium hydrogenation chemistry, thus an evaluation of the electronic structure of known [M(trop$_2$dad)] complexes through their metrical oxidation states was deemed interesting. Some of these complexes in their singlet spin state ($S = 0$) are known to contain significant multireference character to their electronic structures,[17] thus complicating the DAD ligand oxidation state assignment. We therefore sought to combine the information gained from MOS analysis with inexpensive fractional occupation density (FOD) analysis on the crystal structures of these complexes (see Table 4). FOD calculations probe multi-reference character in the electronic ground state arising from static electron correlation between metal and ligand centered (partially) occupied and unoccupied molecular orbitals (see supporting information S5 for details). Many singlet spin state ($S = 0$) [M(trop$_2$dad)] complexes show multi-reference contributions to their ground state wavefunction and were shown to be best described with resonance structures involving ligand oxidation states between DAD^0 and DAD^{2-}, and/or DAD^{1-} contributions (see Figure 1A). In good agreement, our MOS calculator predicts fractional oxidation state values for many of these complexes.

Table 4. MOS and N_{FOD} analysis of various [M(trop$_2$dad)] complexes

Entry	CSD ID	Spin	Molecular Formula	N_{FOD}	MOS
1	HEVWOW	$S = 0$	[Ru(trop$_2$dad)(H)]$^-$	0.78	–1.22
2	YARYAU	$S = 0$	[Ru(trop$_2$dad)(H)]$^-$	0.83	–1.35
3	HEZXIW	$S = 0$	[Ru(trop$_2$dad)(thf)]	0.97	–0.91

4	HEVXIR	S = 0	[Ru(trop$_2$dad)(PPh$_3$)]	0.87	–1.16
5	IKUFOJ	S = 0	[Rh(trop$_2$dad)]$^+$	0.90	–0.24
6	JUXPAV	S = 0	[Fe(trop$_2$dad)(CH$_3$CN)]	1.02	–0.97
7	JUXPEZ	S = 0	[Fe(trop$_2$dad)(PPh$_3$)]	1.12	–0.96
8	JUXPID	S = 0	[Fe(trop$_2$dad)(P(OMe)$_3$)]	0.82	–0.97

From the FOD analysis is clear that all of these singlet (S = 0) ground state complexes indeed have a large (probability of having) multireference character (Table 4, entries 2-4), which is strongly indicative for substantial π-delocalization, metal-to-ligand (single) electron transfer and/or metal-ligand biradical character. The large N_{FOD} values correspond to DAD π-type 'hot electrons' in the FOD plots, thus confirming substantial π-electron delocalization contributions. This can be described with strong π-back donation (contributions of both DAD^0 and DAD^{2-} to the ground state) and/or formation of a DAD^{1-} ligand antiferromagnetically coupled to a metal-centered spin.[26] Both descriptions result in large N_{FOD} values. However, the absolute N_{FOD} value in itself does not tell us whether these 'hot electrons' are primarily located on the metal or rather at the ligand, and hence does discriminate between relative contributions of DAD^0 and DAD^{2-} ligand oxidation states. For that the MOS is a better measure, and combined MOS and FOD results provide a fast and easy to use method to probe the electronic structure of singlet spin state (S = 0) [M(trop$_2$dad)] complexes.

The electronic structure of most of these [M(trop$_2$dad)] complexes seems to be best described by contributions from both DAD^0 and DAD^{2-} resonance structures (Figure 1a) leading to a fractional MOS close to –1.[27,28] The results in Table 4 suggest that for some complexes the DAD^{2-} resonance structure dominates somewhat over DAD^0 (entries 1 and 2), while for others they contribute nearly equally (DAD^{1-}) (entries 3 and 4).[26] For [Rh(trop$_2$dad)]$^+$ the DAD^0 resonance structure clearly dominates (entry 5), which makes sense given the cationic charge of the complex and the higher electronegativity of Rh. Notably, for all three neutral, formally Fe(0) complexes [Fe(trop$_2$dad)(L)] in Table 4 the metrical oxidations states are almost exactly –1, regardless of ligand L. This suggests that these systems are perhaps best described as DAD^{1-} ligands that are (strongly) anti-ferromagnetically coupled to Fe(I)-based spins, but equal contributions of DAD^0 and DAD^{2-} resonance structures cannot be fully excluded.[26] In any case, the FOD analysis results support the robustness of the MOS calculator, thus allowing an accurate description of the ligand oxidation state even in difficult cases with strong static electron correlation effects.

4. Conclusions

The relationship between ligand oxidation state and bond lengths of the backbone of the diazabutadiene (DAD) framework has been made quantitative through a metrical oxidation state model similar to the one developed by Brown for amidophenoxides and catecholates. Several descriptors were evaluated to describe the labile coordination of the C=C backbone, and the bond centroid to metal distance was found to be more accurate and precise than the bond angles within the DAD ligand. As a small backbone interaction can already cause a large bending of the ligand, the more continuous nature of the C=C to metal distance better describes the highly flexible interaction. From the statistical analysis the average C=C→M distance for π-coordination of the enediamide ligand was found to be 2.33 ± 0.07 Å. The developed model was subsequently used successfully on complexes with metals not contained in the training set, showing the generality of the MOS model. Investigation of a single chromium(II) complex with DAD ligands in the −1.5 oxidation state shows that deviations of more than 0.3 from an integer MOS value indicate a deviation from an integer physical oxidation state. The combination of FOD calculations and MOS analysis provides insight into complexes with strong π-backdonation and/or open-shell electronic structures, and as such the MOS calculator was shown to accurately describe the ligand oxidation states even for difficult cases with strong static electron correlation effects. The MOS calculator thus provides a fast and accessible tool to understand the electronic structure of several DAD complexes.

ASSOCIATED CONTENT

Supporting Information.

The following files are available free of charge.

MOS data and calculator (XLSX)

Geometric parameter fits and tabulated data (PDF)

AUTHOR INFORMATION

Corresponding Author

*b.debruin@uva.nl

ORCID

Bas de Bruin: 0000-0002-3482-7669

Felix de Zwart: 0000-0002-0981-1120

Vivek Sinha: 0000-0002-6856-9469

Author Contributions

The manuscript was written through contributions of all authors. All authors have given approval to the final version of the manuscript. VS carried out DFT calculations and FOD analysis.

Notes

The authors declare no competing financial interest.

ACKNOWLEDGMENT

This work was financially supported by the Advanced Research Center for Chemical Building Blocks (ARC-CBBC, project 2018.015.C) which is co-financed by the Netherlands Organization for Scientific Research (NWO). We thank Nicole S. van Leeuwen for useful discussions and support.

SYNOPSIS

Assigning oxidation states to metals and ligands is an important tool for understanding and predicting chemical reactivity. For complexes containing redox-noninnocent ligands, the oxidation state of the ligand can be ambiguous. We present a metrical oxidation state model for 1,4-diazabutadiene ligands, correlating the intra-ligand bond lengths to the oxidation state using information from X-ray structures. This model accounts for the difference in bond length distances between the different coordination modes of the fully reduced ligand.

Graphical Abstract

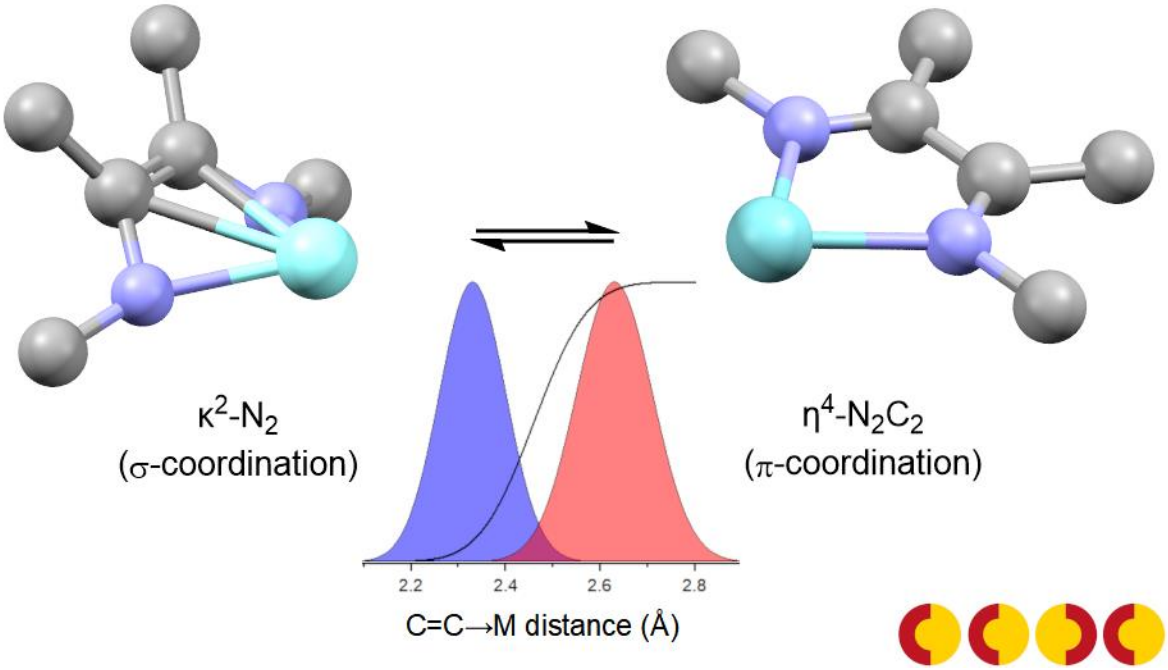

References

---

(1) Jorgensen, C. K., *Oxidation numbers and oxidation states*; Springer Science & Business Media: Berlin, DE, 2012.

(2) Lyaskovskyy, V.; De Bruin, B. Redox Non-Innocent Ligands: Versatile New Tools to Control Catalytic Reactions. *ACS Catal.* **2012**, *2 (2)*, 270–279.

(3) Steinborn, D. The Concept of Oxidation States in Metal Complexes. *J. Chem. Educ.* **2004**, *81* (8), 1148-1154.

(4) Butschke, B.; Fillman, K. L.; Bendikov, T.; Shimon, L. J. W.; Diskin-Posner, Y.; Leitus, G.; Gorelsky, S. I.; Neidig, M. L.; Milstein, D. How Innocent Are Potentially Redox Non-Innocent Ligands? Electronic Structure and Metal Oxidation States in Iron-PNN Complexes as a Representative Case Study. *Inorg. Chem.* **2015**, *54* (10), 4909–4926.

(5) Léonard, N. G.; Yruegas, S.; Ho, S. C.; Sattler, A.; Bezdek, M. J.; Chirik, P. J. Synthesis of Cationic, Dimeric α-Diimine Nickel Hydride Complexes and Relevance to the Polymerization of Olefins. *Organometallics* **2020**, *39* (14), 2630–2635.

(6) Cole, J. C.; Wiggin, S.; Stanzione, F. New Insights and Innovation from a Million Crystal Structures in the Cambridge Structural Database. *Struct. Dyn.* **2019**, *6* (5), 054301.

(7) Taylor, R.; Wood, P. A. A Million Crystal Structures: The Whole Is Greater than the Sum of Its Parts. *Chem. Rev.* **2019**, *119* (16), 9427–9477.

(8) Rahim, A.; Saha, P.; Jha, K. K.; Sukumar, N.; Sarma, B. K. Reciprocal Carbonyl–Carbonyl Interactions in Small Molecules and Proteins. *Nat. Commun.* **2017**, *8* (1).

(9) Reid, R. C.; Yau, M.-K.; Singh, R.; Lim, J.; Fairlie, D. P. Stereoelectronic Effects Dictate Molecular Conformation and Biological Function of Heterocyclic Amides. *J. Am. Chem. Soc.* **2014**, *136* (34), 11914–11917.

(10) Bauzá, A.; Mooibroek, T. J.; Frontera, A. The Bright Future of Unconventional σ/π-Hole Interactions. *ChemPhysChem* **2015**, *16* (12), 2496–2517.

(11) Riniker, S.; Landrum, G. A. Better Informed Distance Geometry: Using What We Know To Improve Conformation Generation. *J. Chem. Inf. Model.* **2015**, *55* (12), 2562–2574.

(12) Welch, A. What Can We Learn from the Crystal Structures of Metallacarboranes? *Crystals* **2017**, *7* (8), 234.

(13) Magubane, M. N.; Nyamato, G. S.; Ojwach, S. O.; Munro, O. Q. Structural, Kinetic, and DFT Studies of the Transfer Hydrogenation of Ketones Mediated by (Pyrazole)Pyridine Iron(II) and Nickel(II) Complexes. *RSC Adv.* **2016**, *6* (69), 65205–65221.

(14) Budzelaar, P. H. M.; De Bruin, B.; Gal, A. W.; Wieghardt, K.; van Lenthe, J. H. Metal-to-Ligand Electron Transfer in Diiminopyridine Complexes of Mn−Zn. A Theoretical Study. *Inorg. Chem.* **2001**, *40* (18), 4649–4655.

(15) Brown, S. N. Metrical Oxidation States of 2-Amidophenoxide and Catecholate Ligands: Structural Signatures of Metal–Ligand π Bonding in Potentially Noninnocent Ligands. *Inorg. Chem.* **2012**, *51* (3), 1251–1260.

(16) Cameron, L. A.; Ziller, J. W.; Heyduk, A. F. Near-IR Absorbing Donor–Acceptor Ligand-to-Ligand Charge-Transfer Complexes of Nickel(II). *Chem. Sci.* **2016**, *7* (3), 1807–1814.

(17) Sinha, V.; Trincado, M.; Grützmacher, H.; de Bruin, B. DFT Provides Insight into the Additive-Free Conversion of Aqueous Methanol to Dihydrogen Catalyzed by [Ru(trop2dad)]: Importance of the (Electronic) Flexibility of the Diazadiene Moiety. *J. Am. Chem. Soc.* **2018**, *140* (40), 13103–13114.

(18) Nishiyama, H.; Ikeda, H.; Saito, T.; Kriegel, B.; Tsurugi, H.; Arnold, J.; Mashima, K. Structural and Electronic Noninnocence of α-Diimine Ligands on Niobium for Reductive C-Cl Bond Activation and Catalytic Radical Addition Reactions. *J. Am. Chem. Soc.* **2017**, *139*, 6494–6505.

(19) Allen, F. H. The Cambridge Structural Database: A Quarter of a Million Crystal Structures and Rising. *Acta. Crystallogr., Sect. B: Struct. Sci.* **2002**, *58* (3), 380–388.

(20) Bruno, I. J.; Cole, J. C.; Edgington, P. R.; Kessler, M.; Macrae, C. F.; McCabe, P.; Pearson, J.; Taylor, R. New Software for Searching the Cambridge Structural Database and Visualizing Crystal Structures. *Acta. Crystallogr., Sect. B: Struct. Sci.* **2002**, *58* (3), 389–397.

(21) One semiiminato (−1) structure with a coordinated backbone was found, CCDC ID: 971183.

(22) Lorenz, V.; Hrib, C. G.; Grote, D.; Hilfert, L.; Krasnopolski, M.; Edelmann, F. T. Diazadiene Complexes of the Heavy Alkaline-Earth Metals Strontium and Barium: Structures and Reactivity. *Organometallics* **2013**, *32* (16), 4636–4642.

(23) Trifonov, A. A.; Borovkov, I. A.; Fedorova, E. A.; Fukin, G. K.; Larionova, J.; Druzhkov, N. O.; Cherkasov, V. K. Ytterbocenes as One- and Two-Electron Reductants in Their

Reactions with Diazadienes: YbIII Mixed-Ligand Bent-Sandwich Complexes Containing a Dianion of Diazabutadiene. *Chem. Eur. J.* **2007**, *13* (17), 4981–4987.

(24) Kreisel, K. A.; Yap, G. P. A.; Theopold, K. H. Synthesis, Characterization, and Electronic Structure of Diimine Complexes of Chromium. *Inorg. Chem.* **2008**, *47* (12), 5293–5303.

(25) CCDC identifiers: QASREJ, NAYSUD, EFEFIF, EFEFUR, KIZXOI.

(26) In a post-HF configuration interaction description, an electronic structure with nearly equal contributions of DAD^0 and DAD^{2-} resonance structures is basically indistinguishable from an electronic structure described as a singlet biradical in which a DAD^{1-} ligand is anti-ferromagnetically (AF) coupled to a metal-based spin (a situation being the result of metal-to-ligand SET). For systems with large AF-coupling constants (large $\Delta E_{S\text{-}T} > 0$) distinguishing between such singlet biradical and strong π-back donation descriptions is (experimentally) impossible and is thus largely a matter of semantics.

(27) Lichtenberg, C.; Adelhardt, M.; Gianetti, T.L.; Meyer, K.; De Bruin, B.; Grützmacher, H. Low-Valent Iron Mono-Diazadiene Compounds: Electronic Structure and Catalytic Application *ACS Catal.*, **2015**, *5*, 6230–6240.

(28) Sinha, V.; Pribanic, B.; De Bruin, B.; Trincado, M.; Grützmacher, H. Ligand- and Metal-Based Reactivity of a Neutral Ruthenium Diolefin Diazadiene Complex: The Innocent, the Guilty and the Suspicious *Chem. – A Eur. J.*, **2018**, *24*, 5513–5521.